Evaluation of dynamic off-resonance correction of respiratory instability in MRI signals for high-order spherical harmonic basis set and multivariate modeling of respiratory sources

Marta Bianciardi[1], Jonathan R Polimeni[1], Kawin Setsompop[1], Cornelius Eichner[1], Berkin Bilgic[1], and Lawrence L Wald[1]

[1]*Department of Radiology, A.A. Martinos Center for Biomedical Imaging, MGH, Harvard Medical School, Boston, MA, United States*

Target Audience: Researches interested in dynamic off-resonance correction of respiratory instability in structural and functional images.

Introduction: Chest motion due to respiration produces off-resonance (OR) B_0 effects in the brain (Fig. 1). OR effects generate blurring, ghosting, and signal instability in both structural and functional MRI, and are a major confound to investigate tissue susceptibility and relaxivity, especially at high magnetic field strength and in deep brain regions. Previous work [1] demonstrated the benefits of dynamic correction of OR effects in the brain due to respiration, by estimating these effects during a calibration scan. In [1], spatial correction was carried out up to the second order, and by the use of a univariate temporal respiratory model.

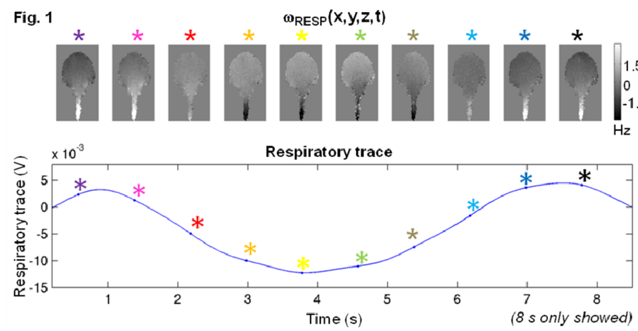

Purpose: To evaluate dynamic OR-correction for increased degrees-of-freedom in both spatial and temporal domain, by employing high-order (up to the fifth) spatial model and multivariate temporal model of respiratory sources.

Methods: Three subjects (2m/1f, age 25 ± 2) participated in the IRB-approved study. The calibration scan was performed at 7 Tesla using GE-EPI, 32 receive-only coil elements and parameters: echo-time = 29 ms, repetition time (TR) = 800 ms, flip angle = 48°, N. slices = 15, slice orientation = sagittal, voxel-size = 2.5×2.5×2.5 mm^3, N. scans: 160, no in-plane acceleration. Chest motion due to respiration was recorded by a piezoelectric respiratory bellow at 1 kHz; the recorded signal was sampled at each slice TR to yield a respiratory time-course (resp(t)). Phase EPI data (Φ) were unwrapped over time after removal of the first image from each time-point, then high-pass filtered (cut-off frequency = 0.1 Hz), and finally converted to frequency shifts ($\omega=\Phi/(2\pi TE)$, Hz) to yield frequency shift signals mainly containing respiratory related changes $\omega_{RESP}(x,y,z,t)$ (example data-set in Fig. 1, coronal slice acquisition). The dynamic OR correction was then performed in two steps:

1) Slice-by-slice least-square fitting of $\omega_{RESP}(x,y,z,t)$ to a multi-variate model of dynamic OR effects ($[Resp_1(t) \ldots Resp_C(t) \ldots Resp_{Nc}(t)]$), which includes multiple ($n = N_C$) sources of respiratory effects, to estimate spatial amplitude maps $A_C(x,y,z)$ of OR effects due to each source C:

$$\omega_{RESP}(x,y,z,t) = \Sigma_C\,[A_C(x,y,z)\cdot Resp_C(t)] + A_0(x,y,z) + \varepsilon_1(x,y,z,t); \qquad C = 1, \ldots, N_c \qquad \text{[Eq. 1]}$$

2) Least-square fitting of each $A_C(x,y,z)$ to a 3D spherical harmonic basis function set $[F_0(x,y,z)\ F_1(x,y,z) \ldots F_m(x,y,z) \ldots F_M(x,y,z)]$ of order up to M, to estimate scalar fitting $\beta_{C,m}$ coefficients to be used during prospective off-resonance correction ($\beta_{C,m}$ are directly related to shim currents values):

$$A_C(x,y,z) = \Sigma_m\,[\beta_{C,m}\cdot F_m(x,y,z)] + \varepsilon_C(x,y,z) \qquad m = 0, \ldots, M;\ \forall\ C = 1, \ldots, N_c \qquad \text{[Eq. 2]}$$

$A_0(x,y,z)$ is the amplitude map of static OR effects, ε_1 and ε_c are noise terms. Note that, we assume that for $M = \infty$ the spherical harmonic basis set fully explains each amplitude map $A_C(x,y,z)$. In the current study, we investigated the use of a bivariate model including both the respiratory time-course ($Resp_1(t) = resp(t)$) and the derivative of resp(t) over time ($Resp_2(t) = d(resp(t))/dt$)), and compared this model's performance to the previous implementation [1] using only $Resp_1(t) = resp(t)$. We also studied the use of a 0–5th order spherical harmonic set, extending previous work [1] employing order 0–2 only. Then the residue after fitting was computed as follows:

$$\omega_{RESIDUE}(x,y,z,t) = \omega_{RESP}(x,y,z,t) - \Sigma_C\,[\Sigma_m\,[\beta_{C,m}\cdot F_m(x,y,z)]\cdot Resp_C(t)] - A_0(x,y,z) \qquad C = 1,\ldots,N_c;\ m = 0,\ldots,M \qquad \text{[Eq. 3]}$$

and the amplitude A and the phase α of $\omega_{RESIDUE}$ (Eq. 3) at the respiratory peak was evaluated in the Fourier domain. For each voxel, A was multiplied by $\sin(\alpha)$ (to retain the sign information), to obtain a measure (ω_{Rpeak}, Hz) of the amount of residual signal fluctuations at the respiratory peak (Rpeak) after dynamic OR correction. A histogram of ω_{Rpeak} was then generated for all voxels inside the brain, and the $FWHM_{Rpeak}$ of a fitted Gaussian function was employed as merit criterion of the dynamic OR correction. $FWHM_{Rpeak}$ was computed for C =1,2 and m=0,5 (this can be employed in both retrospective and prospective OR correction), and also for the special case of $m = \infty$ (this corresponds to using $A_C(x,y,z)$ instead of $\Sigma_m\,[\beta_{C,m}\cdot F_m(x,y,z)]$ in Eq. 3, and can be employed in retrospective OR correction only).

Results: For an example data-set, the spatial distribution (1 slice only) and the histogram of ω_{Rpeak} across the whole brain before and after dynamic OR correction are shown in Fig. 2A and B, respectively. With increasing the spatial model order M, $FWHM_{Residue}$ (shown inside the panels in Fig. 2B, mean (s.e.) across subjects) decreased ($p < 0.05$) for M up to 2 and up to 5 for the univariate and the bivariate model correction, respectively. The bivariate model correction outperformed the univariate model correction for M > 0.

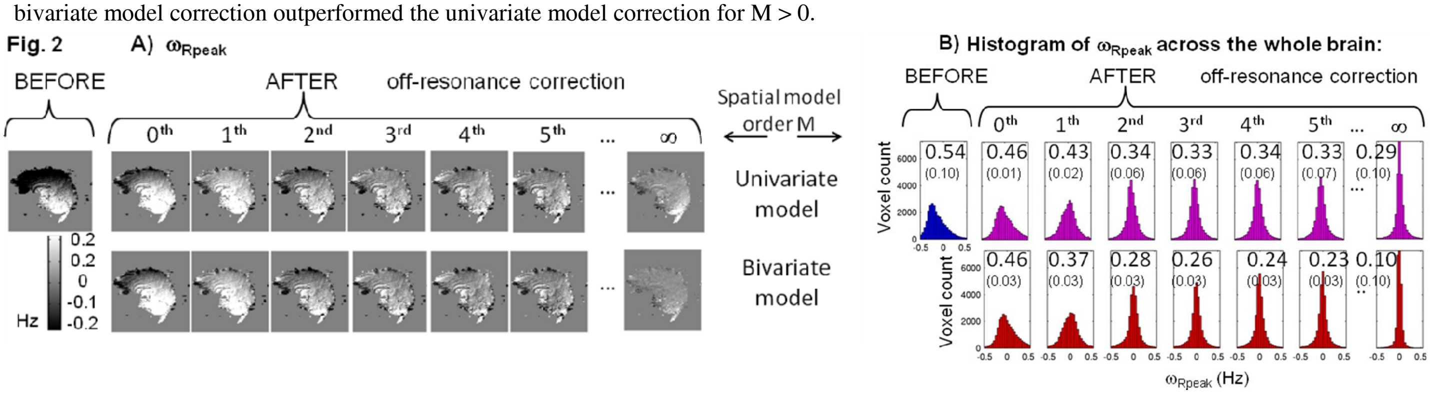

Discussion & Conclusion: Our results demonstrate increased performance of higher-order spatial OR correction and of bivariate compared to univariate temporal modeling of respiratory effects. We are currently investigating the physiological origin of the second modeled source of respiration. These findings also show the expected dynamic capabilities of high-order shim arrays [2] at high magnetic field and on a whole brain basis, including both cortical and subcortical brain regions (e.g. thalamus, brainstem).

References: [1] van Gelderen et al., Magn Reson Med, 57:362-8, 2007. [2] Stockmann et al., Proc. ISMRM, p. 0665, 2013.